I&EC research
Industrial & Engineering Chemistry Research

Article

Cite This: Ind. Eng. Chem. Res. 2019, 58, 9339−9342

pubs.acs.org/IECR

Dissolution Equilibrium and In Situ Growth of HMCM-49 in Aqueous-Phase Reaction

Xinde Sun,* Yingli Wang, Yanli He, Yue Yang, Shutao Xu, Shukui Zhu, Miao Yang, and Zhongmin Liu*

National Engineering Laboratory for Methanol to Olefins, Dalian National Laboratory for Clean Energy, Dalian Institute of Chemical Physics, Chinese Academy of Sciences, Dalian 116023, P. R. China

Supporting Information

ABSTRACT: Insufficient stability of zeolite is one of the key challenges for application of zeolites in aqueous-phase reactions. In long-term catalytic tests on hydrolysis of ethylene glycol monomethyl ether to ethylene glycol, we found that dissolution of HMCM-49 catalysts could lead to complete transformation to kaolinite. Existence of dissolution equilibriums of Si and Al was demonstrated. In situ growth of HMCM-49 occurred where Si concentration in bulk phase surpasses equilibrium value. This almost completely prevented dissolution and phase transformation of HMCM-49. Dissolution of HZSM-5 catalyst was different. A method by dissolving Si and Al in feed is proposed to solve the problem of zeolite stability in aqueous-phase reactions.

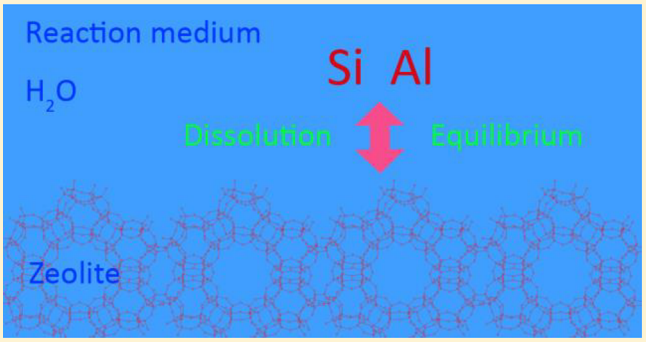

Zeolites are important and widely used catalytic materials. Recently, increasing attention has been paid to zeolite-catalyzed aqueous-phase transformation of biomass which is a current focus.[1−4] One of the key challenges is insufficient stability of zeolites in hot liquid water and aqueous-phase reactions.[1−21] The structural collapse was caused by desilication because of hydrolysis of terminal Si−OH groups[2,5−10] with a density of silanol defects as a crucial factor.[7,11,12] Silylation treatment could improve stability of zeolite in hot liquid water[2−4,7,11,12] and aqueous-phase reactions.[2,4,12] Both framework and extraframework Al were found able to inhibit desilication.[5−10,13,14] Presence of organic reactants showed a protective effect against water.[3]

Bell et al. reported a new effective method to synthesize methyl methoxyacetate by vapor-phase carbonylation of dimethoxymethane over zeolite catalyst.[22] This promoted a new route of ethylene glycol (EG) synthesis from syngas for dimethoxymethane can be easily synthesized from methanol and formaldehyde and methyl methoxyacetate can be reduced directly to ethylene glycol monomethyl ether (EGME)[22] which can convert to EG via hydrolysis over HMCM-49[23] or HZSM-5.[24]

In this paper, we found that dissolution of HMCM-49 catalyst was an equilibrium process and we observed in situ growth of HMCM-49 in 2342-h long-term test on hydrolysis of EGME with a fixed-bed reactor.

The temperature profile of a catalyst bed was a parabolic shape (Figure 1) in the long-term test. Figure 2 shows conversion of EGME (X) and selectivity of EG (S_{EG}). After 680 h, T_M (maximum of the T profile) was raised to

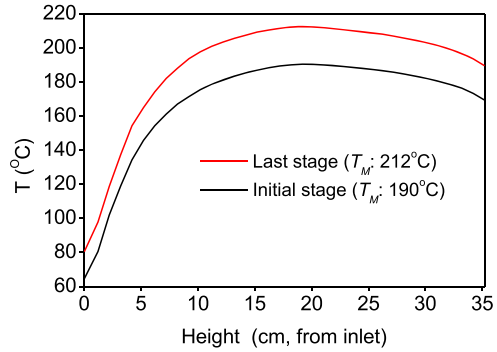

Figure 1. Temperature profiles at initial (T_M = 190 °C) and final (T_M = 212 °C) stage of long-term catalytic testing on EGME hydrolysis.

compensate for loss of catalyst activity and accelerated deactivation was observed. S_{EG} stayed between 42% and 45%. Selectivity of products other than EG was as follows: ethylene glycol dimethyl ether ∼32%, di- and triethylene glycol and their mono- and dimethyl ethers ∼4.3%, dioxane ∼1.5%, methanol ∼12.5%, dimethyl ether ∼3.5%, ethylene epoxide ∼0.3%, and others ∼1%.

Si and Al contents in effluent obtained by ICP analysis are listed in Table 1. Si content increased with temperature. Al content was hundreds times lower than Si and showed no

Received: March 13, 2019
Revised: May 5, 2019
Accepted: May 10, 2019
Published: May 10, 2019

DOI: 10.1021/acs.iecr.9b01417
Ind. Eng. Chem. Res. 2019, 58, 9339−9342

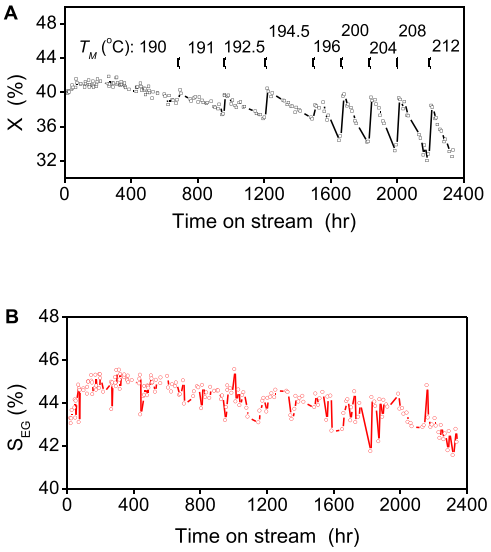

Figure 2. X (A) and S_{EG} (B) of EGME hydrolysis. H_2O/EGME = 4:1 (mol/mol), LHSV = 0.37 mL/g-cat·h, P = 2.0 MPa.

Table 1. Si and Al Contents in Effluents

time on stream (h)	T_M (°C)	T_{outlet} (°C)	Si[a] (mg/L)	Al[a] (mg/L)
48−56	190	170	93	0.35
277−349	190	170	105	0.38
613−685	190	170	105	0.35
960−1039	192.5	172	107	0.36
1416−1495	194.5	174	112	0.30
1663−1759	200	179	119	0.38
1848−1927	204	183	127	0.41
2073−2145	208	186	124	0.37
2337−2342	212	190	124	0.32

[a]Relative error, ±10%.

evident relation with temperature. Total amount of Si and Al in the whole effluent was calculated showing that 32% Si and only 0.17% Al dissolved away from the HMCM-49 catalyst. This prevailing dissolution of Si over Al was consistent with reports that both framework and extraframework Al were able to inhibit desilication in hot liquid water.[5−10,13,14]

The total dissolved Al was only ∼1% of the framework Al in HMCM-49. So, contribution of Al dissolution to deactivation was negligible even if it came from framework Al solely.

The catalyst after testing was separated into eight samples (denoted as A−H, from inlet to outlet). Table 2 shows their results of characterization and catalytic testing.

Si loss (lost Si/primitive Si in catalyst) of the samples was calculated based on Si/Al atom ratios (from XRF) neglecting dissolution of Al (only 0.17% from ICP results). The volume weighted average Si loss was 34% which was consistent with the ICP result (32%). Si loss was high to 66% with samples near the inlet (A and B), though the temperature was low and decreased to negative value (meaning a part of dissolved Si deposited on the samples) near the outlet (G and H) with lower temperature than upstream. It can be concluded that there exists equilibrium of Si between HMCM-49 and liquid bulk phase and the equilibrium concentration of dissolved Si decreases with decreased temperature which was supported by the trend of Si content in effluent with temperature in Table 1. The possible equilibrium of Si dissolution in hot liquid water with HUSY have been mentioned by Ennaert et al.[8] Zeolites

Table 2. Characterization Results of HMCM-49 Catalyst after Testing

sample	$T_{initial}$ (°C)	Si/Al (mol)	Si loss (%)	cryl. (%)	X[a] (%)	kr[b]/cryl.
fresh		1.68		100	21.9	100
A	64−150	0.57	66	34	1.7	21
B	150−176	0.57	66	20	0.9	18
C	176−185	0.94	44	<1	0.2	
D	185−190	1.11	34	<1	0.4	
E	190−188	1.19	29	17	1.1	20
F	188−183	1.4	17	69	5.7	34
G	183−180	1.8	−7	90		
H	180−169	1.9	−13	93	13	55

[a]Tested under the following conditions: H_2O/EGME = 4:1 (mol/mol), T = 195 °C, LHSV = 1.7 mL/mLcat·h, P = 3.0 MPa. [b]Calculated assuming that the reaction order of EGME conversion is 1.5 and the total moles remain unchanged after reaction. Relative error: Si/Al, ±5%; cryl., ±5%; X, ±3%.

are metastable materials usually synthesized in aqueous solution. Dissolution of zeolite in aqueous-phase medium can be considered as the reverse of its synthetic reaction. And the equilibrium moved toward synthetic direction and led to growth of MCM-49 stucture (demonstrated by ^{29}Si MAS NMR data below) on samples G and H.

Combining the Si loss and relative crystallinity (cryl.) data can lead to the conclusion that Si dissolution greatly promoted phase transformation of MCM-49 to kaolinite (XRD patterns, see Figure 3). This is similar to ZSM-22 in hot liquid water.[14]

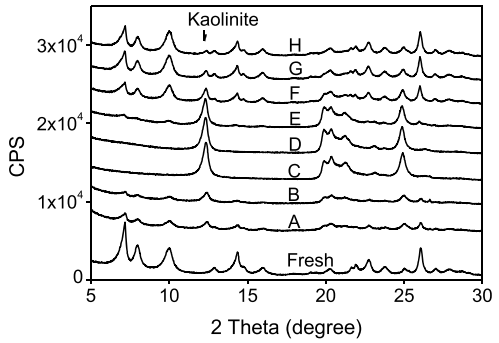

Figure 3. XRD patterns of HMCM-49 catalysts after testing.

The retained crystallinity of samples A and B shows that the phase transformation was quite sensitive to temperature and so have high activation energy. The amazing high crystallinity of samples G and H shows that deposition of Si was very effective to preserve structure of HMCM-49.

The residual catalytic activity of tested samples (except G) was compared to that of fresh catalyst in form of X and kr/cryl. (kr, relative rate constant) in Table 2. Decline in kr/cryl. compared to that of fresh catalyst represents deactivation ascribed to coking. It can be seen that coking and phase transformation of MCM-49 promoted by Si dissolution were the primary reasons for deactivation.

Static dissolution experiment was performed to verify existence of Si dissolution equilibrium. Si loss of the HMCM-49 catalyst was 2.2% based on Si/Al ratio (from XRF) or 6.3% based on Si content in the liquid (195 mg/L, from ICP) after 2000 h at 210 °C. Al loss was 0.02% based on Al content of the liquid (0.31 mg/L, from ICP). They were

DOI: 10.1021/acs.iecr.9b01417
Ind. Eng. Chem. Res. 2019, 58, 9339−9342

about 1 magnitude lower than loss in the long-term catalytic test while Si or Al content in liquid was close. These results verified existence of Si dissolution equilibrium. Furthermore, this also proved existence of Al dissolution equilibrium which may involve Al_2O_3 binder. So, the Si and Al contents in Table 1 were their equilibrium concentrations at T_{outlet} in EGME hydrolysis effluent except for the last stages. Relative crystallinity of the HMCM-49 after static experiment declined to 71%. The decline is more severe than expected from the relationship between Si loss and cryl. at lower temperature shown in Table 2. This supports the foregoing conclusion that transformation of MCM-49 was sensitive to temperature.

Figure 4 shows ^{29}Si MAS NMR spectra of fresh and tested catalysts. The resonance at −91.5 ppm can be assigned to Si

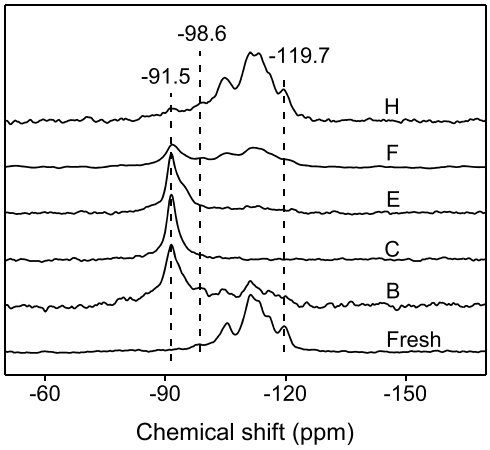

Figure 4. ^{29}Si MAS NMR spectra of fresh and tested HMCM-49 catalysts.

(4Al) of kaolinite structure based on the foregoing XRD results and ref 25. Resonances at −98.6 to −119.7 ppm are assigned to MCM-49 framework with Q3 or Si (2Al) environment at −98.6 ppm, Si (1Al) environment around −105 ppm, and Si (0Al) environment at −109 to −119.7 ppm. The relative resonance intensities of kaolinite and MCM-49 are consistent with the XRD results.

Decomposition and assignment of ^{29}Si NMR spectrum over sample H is shown in Figure S1 and Table S1 in the Supporting Information. The Si assigned to MCM-49 framework reaches 95.4% in the total Si. This shows that in situ growth of MCM-49 was achieved and the increased MCM-49 structure corresponded to 60% of Si deposited on sample H. It is probable that all deposited Si formed MCM-49 structure while transformation to kaolinite occurred slightly which was a parallel process with equilibrium of dissolution and in situ growth of MCM-49 as proposed with HBEA zeolite.[5]

Other decomposition results show that the portion of Si connected to Al (at −98.6 to −106.2 ppm) in total framework Si is 47% on sample B with severe Si loss, much higher than fresh catalyst (19%). This demonstrates that Al in HMCM-49 played the role as a stabilizer to connected Si atoms. It is in agreement with reports in hot liquid water.[5,8−10] The value of sample H (32%) was also higher than that of fresh catalyst. This shows that the in situ grown MCM-49 structure came from both Si and Al dissolved in bulk phase in a ratio less than the primary zeolite and hints that the dissolved Al was likely from binder Al_2O_3.

In summary, collapse of HMCM-49 in this aqueous reaction involves two consecutive steps. The first is dissolution of Si from the zeolite framework which engenders defects[5,9,10] and is confined by dissolution equilibrium. The second is transformation to kaolinite which is promoted greatly by the first step (maybe due to the formed defects[7,11,12]) and would be stopped by in situ growth of MCM-49—reverse of dissolution. Meanwhile, the transformation also occurs in parallel at a slow rate. This is somewhat different from the decomposition mechanism of HBEA in hot water proposed by Lercher et al.[5]

HZSM-5 is also effective catalyst for EGME hydrolysis.[24] Dissolution of HZSM-5 catalyst was compared to HMCM-49 during catalytic testing under H_2O/EGME = 4:1 (mol/mol), T = 184 °C, LHSV = 1.5 mL/g-cat·h, and P = 3.0 MPa. Dissolution rates (dissolved Si per hour/primitive Si in catalyst) were calculated based on Si contents (62.6 mg/L for HZSM-5, 121 mg/L for HMCM-49) and Al contents (0.12 mg/L for HZSM-5, 0.13 mg/L for HMCM-49) in reaction effluents by ICP analysis. The results show that Si dissolution rate of HZSM-5 (2.6×10^{-4} h^{-1}) was less than half of HMCM-49 (5.9×10^{-4} h^{-1}) while the order was the reverse with Al dissolution rate (1.5×10^{-6} h^{-1} for HZSM-5, 1.0×10^{-6} h^{-1} for HMCM-49). This shows that dissolution is quite different with different zeolite. The catalytic performance of HZSM-5/HMCM-49 was as follows: EGME conversion 12.9/17.5%; selectivity of EG 35.9/39.2%, ethylene glycol dimethyl ether 44.3/40.8%, di- and triethylene glycol and their mono- and dimethyl ethers 10.1/5.9%, dioxane 0.2/0.6%, methanol 8.1/11.7%, dimethyl ether 0.5/0.9%, ethylene epoxide 0.4/0.3%, and others 0.5/0.6%.

On the basis of dissolution equilibrium, which should be valid with other zeolites and aqueous reactions, a simple and prospective method is proposed to avoid dissolution of zeolite in aqueous-phase reactions and match the long lifetime requirement of industrialization. It is to dissolve Si and Al at definite concentration in the feed. In situ growth of zeolite can be achieved when the concentration is higher than equilibrium value. The samples G and H demonstrated amazing effectiveness.

■ ASSOCIATED CONTENT

Supporting Information

The Supporting Information is available free of charge on the ACS Publications website at DOI: 10.1021/acs.iecr.9b01417.

Experimental procedure, calculation method of dissolution rate, figure, table, and refs 1−3 (PDF)

■ AUTHOR INFORMATION

Corresponding Authors

*E-mail: sunxd@dicp.ac.cn (X.S.).
*E-mail: liuzm@dicp.ac.cn (Z.L.).

ORCID

Xinde Sun: 0000-0003-0874-0460
Shutao Xu: 0000-0003-4722-8371
Zhongmin Liu: 0000-0002-7999-2940

Notes

The authors declare no competing financial interest.

■ ACKNOWLEDGMENTS

We are grateful to Xinxin Lv, Liang Wang, Liang Qi, and Linying Wang for their help with experiments and beneficial

DOI: 10.1021/acs.iecr.9b01417
Ind. Eng. Chem. Res. 2019, 58, 9339−9342

discussions. The authors are grateful for funding from the National Natural Science Foundation of China (Grant No. 21878287).

REFERENCES

(1) Ennaert, T.; Van Aelst, J.; Dijkmans, J.; De Clercq, R.; Schutyser, W.; Dusselier, M.; Verboekend, D.; Sels, B. F. Potential and challenges of zeolite chemistry in the catalytic conversion of biomass. *Chem. Soc. Rev.* **2016**, *45*, 584−611.
(2) Prodinger, S.; Shi, H.; Eckstein, S.; Hu, J. Z.; Olarte, M. V.; Camaioni, D. M.; Derewinski, M. A.; Lercher, J. A. Stability of zeolites in aqueous phase reactions. *Chem. Mater.* **2017**, *29*, 7255−7262.
(3) Zapata, P. A.; Huang, Y.; Gonzalez-Borja, M. A.; Resasco, D. E. Silylated hydrophobic zeolites with enhanced tolerance to hot liquid water. *J. Catal.* **2013**, *308*, 82−97.
(4) Zapata, P. A.; Faria, J.; Ruiz, M. P.; Jentoft, R. E.; Resasco, D. E. Hydrophobic zeolites for biofuel upgrading reactions at the liquid-liquid interface in water/oil emulsions. *J. Am. Chem. Soc.* **2012**, *134*, 8570−8578.
(5) Vjunov, A.; Fulton, J. L.; Camaioni, D. M.; Hu, J. Z.; Burton, S. D.; Arslan, I.; Lercher, J. A. Impact of aqueous medium on zeolite framework integrity. *Chem. Mater.* **2015**, *27*, 3533−3545.
(6) Ravenelle, R. M.; Schüßler, F.; D'Amico, A.; Danilina, N.; van Bokhoven, J. A.; Lercher, J. A.; Jones, C. W.; Sievers, C. Stability of zeolites in hot liquid water. *J. Phys. Chem. C* **2010**, *114*, 19582−19595.
(7) Zhang, L.; Chen, K.; Chen, B.; White, J. L.; Resasco, D. E. Factors that determine zeolite stability in hot liquid water. *J. Am. Chem. Soc.* **2015**, *137*, 11810−11819.
(8) Ennaert, T.; Geboers, J.; Gobechiya, E.; Courtin, C. M.; Kurttepeli, M.; Houthoofd, K.; Kirschhock, C. E. A.; Magusin, P. C. M. M.; Bals, S.; Jacobs, P. A.; Sels, B. F. Conceptual frame rationalizing the self-stabilization of H-USY zeolites in hot liquid water. *ACS Catal.* **2015**, *5*, 754−768.
(9) Shen, S. C.; Kawi, S. Understanding of the effect of Al substitution on the hydrothermal stability of MCM-41. *J. Phys. Chem. B* **1999**, *103*, 8870−8876.
(10) Mokaya, R. Al content dependent hydrothermal stability of directly synthesized aluminosilicate MCM-41. *J. Phys. Chem. B* **2000**, *104*, 8279−8286.
(11) Prodinger, S.; Derewinski, M. A.; Vjunov, A.; Burton, S. D.; Arslan, I.; Lercher, J. A. Improving stability of zeolites in aqueous phase via selective removal of structural defects. *J. Am. Chem. Soc.* **2016**, *138*, 4408−4415.
(12) Prodinger, S.; Shi, H.; Wang, H.; Derewinski, M. A.; Lercher, J. A. Impact of structural defects and hydronium ion concentration on the stability of zeolite BEA in aqueous phase. *Appl. Catal., B* **2018**, *237*, 996−1002.
(13) Lutz, W.; Gessner, W.; Bertram, R.; Pitsch, I.; Fricke, R. Hydrothermally resistant high-silica Y zeolites stabilized by covering with non-framework aluminum species. *Microporous Mater.* **1997**, *12*, 131−139.
(14) Jamil, A. K.; Muraza, O.; Osuga, R.; Shafei, E. N.; Choi, K. H.; Yamani, Z. H.; Somali, A.; Yokoi, T. Hydrothermal stability of one-dimensional pore ZSM-22 zeolite in hot water. *J. Phys. Chem. C* **2016**, *120*, 22918−22926.
(15) Buhl, J. C.; Herzog, T.; Lutz, W.; Wieprecht, W. Z. Phase transformation of hydrothermally stressed adsorbents. *Z. Anorg. Allg. Chem.* **2018**, *644*, 1078−1083.
(16) Bakare, I. A.; Muraza, O.; Kurniawan, T.; Yamani, Z. H.; Shafei, E. N.; Punetha, A. K.; Choi, K. H.; Yokoi, T. Hydrothermal stability of MTT zeolite in hot water: The role of La and Ce. *Microporous Mesoporous Mater.* **2016**, *233*, 93−101.
(17) Vjunov, A.; Derewinski, M. A.; Fulton, J. L.; Camaioni, D. M.; Lercher, J. A. Impact of zeolite aging in hot liquid water on activity for acid-catalyzed dehydration of alcohols. *J. Am. Chem. Soc.* **2015**, *137*, 10374−10382.
(18) Kruger, J. S.; Nikolakis, V.; Vlachos, D. G. Aqueous-phase fructose dehydration using Brønsted acid zeolites: Catalytic activity of dissolved aluminosilicate species. *Appl. Catal., A* **2014**, *469*, 116−123.
(19) Kruger, J. S.; Choudhary, V.; Nikolakis, V.; Vlachos, D. G. Elucidating the roles of zeolite H-BEA in aqueous-phase fructose dehydration and HMF rehydration. *ACS Catal.* **2013**, *3*, 1279−1291.
(20) Lutz, W.; Kurzhals, R.; Sauerbeck, S.; Toufar, H.; Buhl, J. C.; Gesing, T.; Altenburg, W.; Jäger, C. Hydrothermal stability of zeolite SAPO-11. *Microporous Mesoporous Mater.* **2010**, *132*, 31−36.
(21) Lutz, W.; Toufar, H.; Kurzhals, R.; Suckow, M. Investigation and modeling of the hydrothermal stability of technically relevant zeolites. *Adsorption* **2005**, *11*, 405−413.
(22) Celik, F. E.; Kim, T. J.; Bell, A. T. Vapor-phase carbonylation of dimethoxymethane over H-Faujasite. *Angew. Chem., Int. Ed.* **2009**, *48*, 4813−4815.
(23) Sun, X.; Wang, Y.; Zhu, S.; Liu, Z.; Tian, P.; Yang, M.; Yang, Y. A transformation method for ethylene glycol monomethyl ether. C.N. Patent CN107 814 690, 2016.
(24) Ni, Y.; Zhu, W.; Liu, Y.; Liu, H.; Shi, L.; Liu, Z. A method for hydrolysis of ethylene glycol monomethyl ether to ethylene glycol. C.N. Patent CN106 554 250, 2015.
(25) Buhl, J. C.; Hoffmann, W.; Buckermann, W. A.; Muller-Warmuth, W. The crystallization kinetics of sodalites grown by the hydrothermal transformation of kaolinite studied by ^{29}Si MAS NMR. *Solid State Nucl. Magn. Reson.* **1997**, *9*, 121−128.

DOI: 10.1021/acs.iecr.9b01417
Ind. Eng. Chem. Res. 2019, 58, 9339−9342